JOURNAL OF NATURAL PRODUCTS

Article

pubs.acs.org/jnp

Mycoleptones A–C and Polyketides from the Endophyte *Mycoleptodiscus indicus*

Willian J. Andrioli,[†] Raphael Conti,[†] Magali J. Araújo,[‡] Riccardo Zanasi,[§] Bruno C. Cavalcanti,[⊥] Viviane Manfrim,[∥] Juliano S. Toledo,[∥] Daniele Tedesco,[▽] Manoel O. de Moraes,[⊥] Cláudia Pessoa,[⊥] Angela K. Cruz,[∥] Carlo Bertucci,[▽] José Sabino,[○] Dhammika N. P. Nanayakkara,[#] Mônica. T. Pupo,[†] and Jairo K. Bastos*[,†]

[†]Faculdade de Ciências Farmacêuticas de Ribeirão Preto, Universidade de São Paulo, 14040-903, Ribeirão Preto, SP, Brazil

[‡]Departamento de Antibióticos, Universidade Federal do Pernambuco, 50670-901, Recife, PE, Brazil

[§]Department of Chemistry and Biology, University of Salerno, 84084, Fisciano, Italy

[⊥]Departamento de Fisiologia e Farmacologia, Universidade Federal do Ceará, 60430-270, Fortaleza, CE, Brazil

[∥]Faculdade de Medicina de Ribeirão Preto, Universidade de São Paulo, 14040-903, Ribeirão Preto, SP, Brazil

[▽]Department of Pharmacy and Biotechnology, University of Bologna, 40126, Bologna, Italy

[○]Instituto de Física, Universidade Federal de Goiás, 74001-970, Goiânia, GO, Brazil

[#]National Center for Natural Products Research, University of Mississippi, Oxford, Mississippi 38677, United States

Supporting Information

ABSTRACT: Three new azaphilones with an unusual methylene bridge, named mycoleptones A, B, and C (**2**, **4**, and **5**), were isolated from cultures of *Mycoleptodiscus indicus*, a fungus associated with the South American medicinal plant *Borreria verticillata*. Additionally, four known polyketides, austdiol (**1**), eugenitin (**3**), 6-methoxyeugenin (**6**), and 9-hydroxyeugenin (**7**), were also isolated. The structural characterization of compounds was carried out by nuclear magnetic resonance spectroscopy, high-resolution mass spectrometry, electronic circular dichroism spectroscopy, time-dependent density functional theory calculations, and X-ray crystallography. Compounds **1**–**9** were weakly active when tested in antileishmanial and cytotoxicity assays.

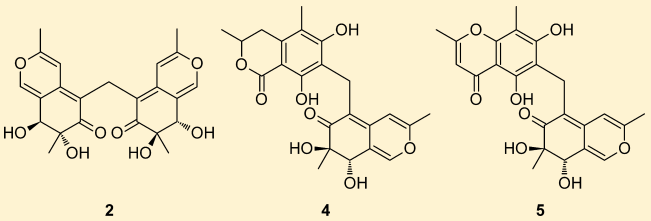

Endophytic microorganisms live inside the tissues of host plants without apparently harming them and are a promising source of bioactive compounds.[1−4] Species of *Mycoleptodiscus*, such as *M. indicus, M. terrestris*, and *M. sphericus*, are commonly isolated as endophytes; they are probably latently phytopathogenic and may become phytopathogenic when the host plant is subjected to stress.[5] *M. indicus*, a tropical to subtropical species, occurs in leaves of different host plants, mainly monocotyledons. *M. indicus* is associated with large spreading lesions on leaves of *Zamia* spp., an American cycad, and other monocotyledonous plants.[6] *M. indicus* has occasionally been reported to infect humans and canines, causing septic arthritis and skin infections.[7]

In this paper, the isolation, structural characterization, and biological activity of secondary metabolites from cultures of *M. indicus,* an endophytic fungus isolated from the leaves from *Borreria verticillata* (Rubiaceae), are reported. Three new azaphilones, named mycoleptones A, B, and C (**2**, **4**, and **5**), were isolated and fully characterized; in addition, four known polyketides, namely, austdiol (**1**), eugenitin (**3**), 6-methoxyeugenin (**6**), and 9-hydroxyeugenin (**7**), were isolated and identified, and the acetylated derivatives of austdiol (**8**) and mycoleptone A (**9**) were synthesized (Figure 1).

RESULTS AND DISCUSSION

Seven secondary metabolites of *M. indicus* were isolated, four of which were identified as austdiol, eugenitin, 6-methoxyeugenin, and 9-hydroxyeugenin by comparison of experimental spectroscopic data with literature values.[8−13] Austdiol ((7*R*,8*S*)-7,8-dihydroxy-3,7-dimethyl-6-oxo-7,8-dihydro-6*H*-isochromene-5-carbaldehyde) is the main toxic component of a mixture of compounds produced in moldy maize meal by *Aspergillus ustus* and belongs to a class of compounds known generically as azaphilones.[14,15] Azaphilones are yellow or orange pigments produced by fungi: their pyran oxygen atoms are easily exchanged to nitrogen atoms with ammonia, and the name is derived from the ready reaction of these metabolites with ammonia to yield vinylogous γ-pyridones.[16] The skeleton of austdiol is derived from a single pentaketide chain, composed of

Received: August 22, 2013
Published: January 3, 2014

dx.doi.org/10.1021/np4006822 | *J. Nat. Prod.* 2014, 77, 70−78

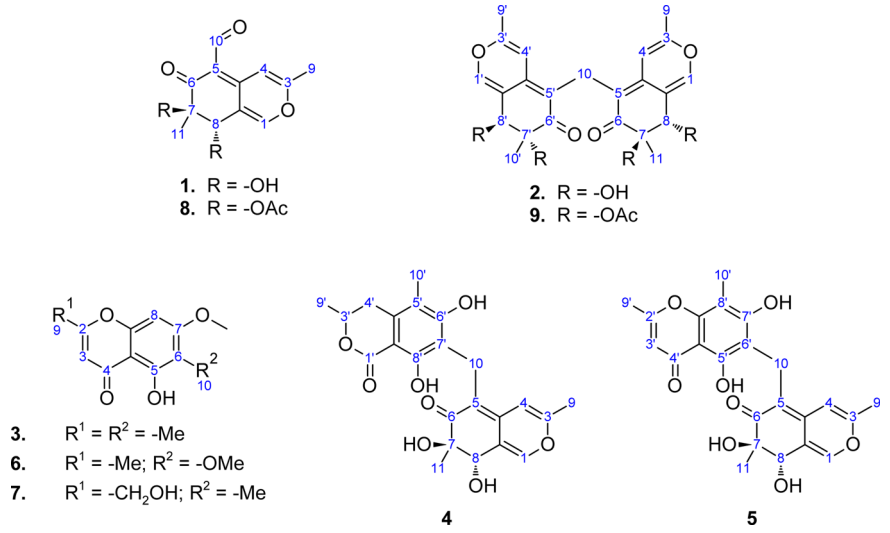

Figure 1. Mycoleptones A–C and polyketides from *Mycoleptodiscus indicus*.

head-to-tail acetate units, and possesses two C_1 units introduced from *S*-adenosylmethionine.[17] A wide range of interesting biological activities of azaphilones, such as antimicrobial, antifungal, antiviral, antioxidant, cytotoxic, nematicidal, and anti-inflammatory, have been reported in the literature;[14,17] their nonselective biological activities may be related to the production of vinylogous γ-pyridones.[18]

Three of the isolated metabolites are previously unreported azaphilones and were named mycoleptones A, B, and C (**2**, **4**, and **5**). Mycoleptone A (**2**) was isolated as a yellow powder, and the complete structural characterization was carried out by nuclear magnetic resonance (NMR) spectroscopy, high-resolution mass spectrometry (HRMS), electronic circular dichroism (ECD) spectroscopy, time-dependent density functional theory (TD-DFT) calculations, and single-crystal X-ray diffraction studies (Figure 2). The UV spectrum of **2** displays maximum absorptions at 254 nm (log ε 2.90) and 361 nm (log ε 2.83), revealing the presence of an extended conjugated system, characteristic of azaphilones. Compound **2** displays similar ^{1}H and ^{13}C NMR spectra to austdiol,[8,9] with the replacement of the aldehyde signals (δ_H 9.99 and δ_C 189.3) by methylene signals (δ_H 3.26 and δ_C 18.5) at position C-5. The ^{1}H NMR spectrum exhibits two signals at δ_H 7.30 and 6.25 due to hydrogen atoms on the pyran ring, two hydroxyl hydrogens at δ_H 5.66 (OH, d, J = 4.6 Hz) and 4.93 (OH, s), a methine signal at δ_H 4.22 (1H, d, J = 4.6 Hz), a methylene signal at δ_H 3.26, and two methyl signals at δ_H 2.07 and 0.91. The ^{13}C NMR spectrum displays signals for 12 carbons atoms, 11 of which refer to two atoms each: two signals due to methyl carbon atoms (δ_C 19.2 and 18.8), five signals from the skeleton of the pyran rings (δ_C 157.8; 143.5; 141.0; 120.7 and 104.6), and four signals from the skeleton of the cyclohexenone, with one signal due to ketone carbonyl groups (δ_C 197.8; IR ν_{max} 1667 cm^{-1}), one due to quaternary unsaturated carbon atoms (δ_C 112.7), and two due to oxygenated carbon atoms (δ_C 75.6 and 71.0). The remaining signal refers to a methylene group (δ_C 18.5). The heteronuclear multiple-bond correlation (HMBC) spectrum shows key correlations of CH_2-10 to C-4a, C-5, C-6, C-4a′, C-5′, and C-6′, revealing the attachment of two azaphilone units through a methylene bridge at position C-5 (Table 1). Furthermore, the presence of four hydroxyl groups was confirmed by acetylation with pyridine–Ac_2O to afford the tetraacetylated derivative (**9**). NMR spectroscopy identifies the structure of **2** as being formed by two austdiol units linked by a methylene group, generating a compound with the molecular formula $C_{23}H_{24}O_8$ as determined by HRMS ($[M + H]^+$ at m/z 429.1543). The chemical structure explains the simplicity of the ^{1}H and ^{13}C NMR spectra, in which the signal intensities are doubled, except for the methylene group.

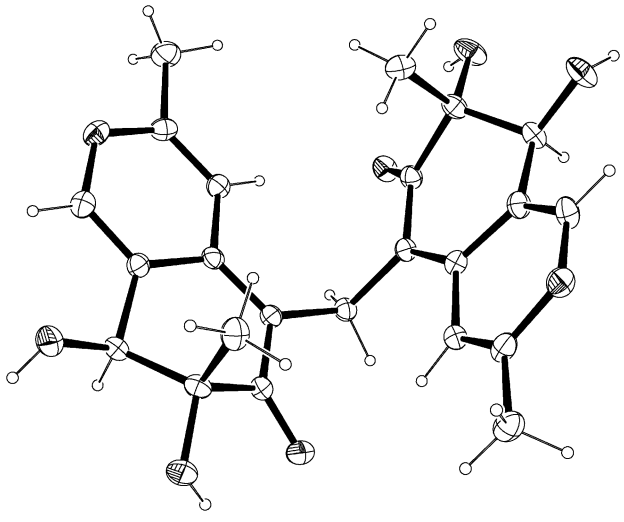

Figure 2. ORTEP representation of mycoleptone A (atom displacement at 30% probability). Hydrogen atoms are represented by spheres of arbitrary radius.

Compound **2** is a chiral molecule having four asymmetric carbons and a formal binary symmetry axis. An accurate analysis of the eight enantiomeric pairs of **2** reveals that two pairs are formed by nonoptically active *meso* structures and two more pairs are repeated twice; as a result, four pairs of enantiomers and two *meso* structures are possible. Since the reliable assessment of the absolute configuration of a compound is achieved when the theoretical chiroptical properties[19] of all the possible optically active diastereomers are determined,[20] quantum-mechanical (QM) calculations were performed on four diastereomers of **2** (Figure 3): (7*R*,8*S*,7′*R*,8′*S*)-**2** (**2A**), (7*R*,8*S*,7′*R*,8′*R*)-**2** (**2B**), (7*R*,8*S*,7′*S*,8′*S*)-**2** (**2C**), and (7*S*,8*S*,7′*S*,8′*S*)-**2** (**2D**). QM calculations were carried out

dx.doi.org/10.1021/np4006822 | J. Nat. Prod. 2014, 77, 70–78

Table 1. NMR Spectroscopic Data (400 MHz) for Mycoleptones A–C

	mycoleptone A (**2**)[a]			mycoleptone B (**4**)[b]			mycoleptone C (**5**)[a]		
position	δ_C mult.	δ_H (J in Hz)	HMBC[c]	δ_C mult.	δ_H (J in Hz)	HMBC[c]	δ_C mult.	δ_H (J in Hz)	HMBC[c]
1	143.5, CH	7.30, s	3, 4a, 8, 8a	144.8, CH	7.43, d (1.8)	3, 4a, 8, 8a	145.7, CH	7.52, s	3, 4a, 8, 8a
2									
3	157.8, C			160.1, C			160.5, C		
4	104.6, CH	6.25, s	3, 4a, 5, 8a, 9	104.4, CH	6.63, s	3, 5, 8a, 9	105.5, CH	7.03, s	3, 8a
4a	141.0, C			143.7, C			144.3, C		
5	112.7, C			112.8, C			112.1, C		
6	197.8, C			199.3, C			200.5, C		
7	75.6, C	4.93, s (OH)		76.1, C			75.4, C		
8	71.0, CH	4.22, d (4.6); 5.66, d (OH) (4.6)	1, 6, 7, 8a, 10	71.5, CH	4.42, d (1.8)	7, 8a, 11	70.7, CH	4.25, s	1, 6, 7, 8a
8a	120.7, C			121.1, C			121.3, C		
9	19.2, CH_3	2.07, s	3, 4	18.3, CH_3	2.22, s	3, 4	19.5, CH_3	2.25, s	3, 4
10	18.5, CH_2	3.26, s	4a, 5, 6, 4a′, 5′, 6′	20.7, CH_2	3.53, 3.60, d (15.0)	4a, 5, 6, 6′, 7′, 8′	18.6, CH_2	3.74, 3.46, d (15.0)	4a, 5, 6, 5′, 6′, 7′
11	18.8, CH_3	0.91, s	6, 7, 8	17.5, CH_3	1.10, s	6, 7	19.0, CH_3	1.00, s	6, 7, 8
1′	143.5, CH	7.30, s	3′, 4a′, 8′, 8a′	171.2, C					
2′							167.2, C		
3′	157.8, C			75.0, CH	4.55, m		107.9, CH	6.13, s	2′, 4a′, 9′
4′	104.6, CH	6.25, s	3′, 4a′, 5′, 8a′, 9′	32.2, CH_2	3.17, dd (16.0, 3.0)	5′, 8a′			
					2.60, dd (16.0, 11.0)	3′, 5′, 8a′, 9′	181.8, C		
4a′	141.0, C			110.1, C			103.1, C		
5′	112.7, C			136.8, C			156.6, C	13.06, s (OH)	4a′, 5′, 6′
6′	197.8, C			160.2, C			107.8, C		
7′	75.6, C	4.93, s (OH)		116.5, C			161.1, C		
8′	71.0, CH	4.22, d (4.6); 5.66, d (OH) (4.6)	1′, 6′, 7′, 8a′, 10′	160.9, C			105.0, C		
8a′	120.7, C			100.1, C			153.5, C		
9′	19.2, CH_3	2.07, s	3′, 4′	19.6, CH_3	1.44, d (6.2)	3′, 4′	20.2, CH_3	2.37, s	2′, 3′
10′	18.8, CH_3	0.91, s	6′, 7′, 8′	6.9, CH_3	2.06, s	4a′, 5′, 6′	8.5, CH_3	2.00, s	7′, 8′, 8a′

[a]In DMSO-d_6. [b]In CD_3OD. [c]HMBC correlations are from hydrogen(s) stated to the indicated carbon.

using density functional theory (DFT) and its time-dependent extension (TD-DFT); detailed results are reported in the Supporting Information. DFT geometry optimization (Table 2) yielded two equilibrium conformers having $\Delta E_{QM} \leq 2$ kcal mol^{-1} for diastereomers **2A**, **2B**, and **2C**, while a single equilibrium conformer within the same threshold energy was found for diastereomer **2D**. The most populated conformers of **2A** (Figure 4) display similar geometric features: the azaphilone units are oriented in an "open folder" conformation, the pyran oxygen atoms are pointing toward opposite directions, and all the hydroxy groups are equatorial and form intramolecular hydrogen bonds with each other and with the ketone carbonyl groups. The main difference lies in the direction of the axial methyl groups on C-7 and C-7′, which point outside the molecular cavity for **2A-e** and inside for **2A-b**.

The experimental ECD spectrum of **2** in methanol (Figure 5) shows four bands. The broad positive band centered at 372 nm has a strong contribution from the n → π* transitions of the ketone carbonyls, which are affected by the chiral environment around these groups. The positive band at 311 nm with a shoulder around 285 nm, the sharp negative peak at 252 nm, and the positive peak at 228 nm are due to π → π* transitions of the conjugated system, which are affected by the chirality of the rings and by the mutual orientation of the azaphilone units. The theoretical ECD spectra of the diastereomers of **2** (Figure 6) displayed different patterns, reflecting their different stereochemistry. The comparison between the calculated spectrum of **2A** and the experimental spectrum of **2** (Figure 7) shows that TD-DFT calculations are able to reproduce the experimental pattern of the transitions in the high-energy region, considering that transition energies are usually underestimated by PBE0.[21] The transitions in the low-energy region are not reproduced, suggesting that QM calculations are unable to describe the chiral environment of the ketone moieties, in particular hydrogen-bonding interactions with hydroxy groups and solvent molecules, with adequate accuracy. On the other hand, the theoretical ECD spectra of the remaining diastereomers (reported in the Supporting Information) are unable to reproduce the experimental ECD pattern in the high-energy region: on this basis, a (7*R*,8*S*,7′*R*,8′*S*) absolute configuration can be predicted for **2**.

Compound **2** crystallizes with two independent molecules in the asymmetric unit (Figure 2); the X-ray geometric parameters selected for comparison with the precursor austdiol are listed in Table 3. The C-5–C-10 distance was elongated upon change of hybridization to sp^3 for atom C-10, and the C-5–C-4a distance was shortened, increasing the double-bond character. The pyran rings are almost planar with an rmsd from the mean plane of 0.03 Å, while the cyclohexenone rings adopt a twisted envelope conformation with atoms C-7 and C-7′ as flap atoms. The X-ray structure of **2** shows that the azaphilone units have the same absolute configuration as austdiol,[22] retaining the stereochemistry of the chiral centers as (7*R*,8*S*); moreover,

dx.doi.org/10.1021/np4006822 | J. Nat. Prod. 2014, 77, 70–78

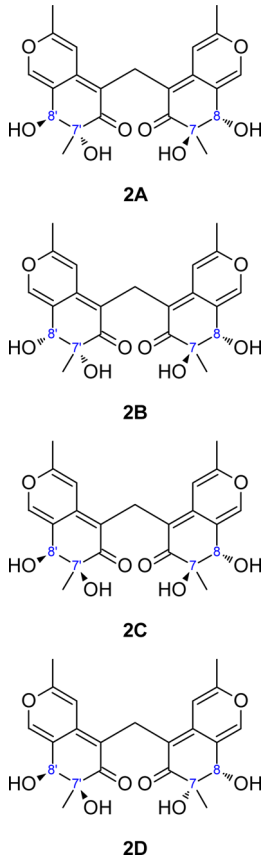

Figure 3. Diastereomers of mycoleptone A.

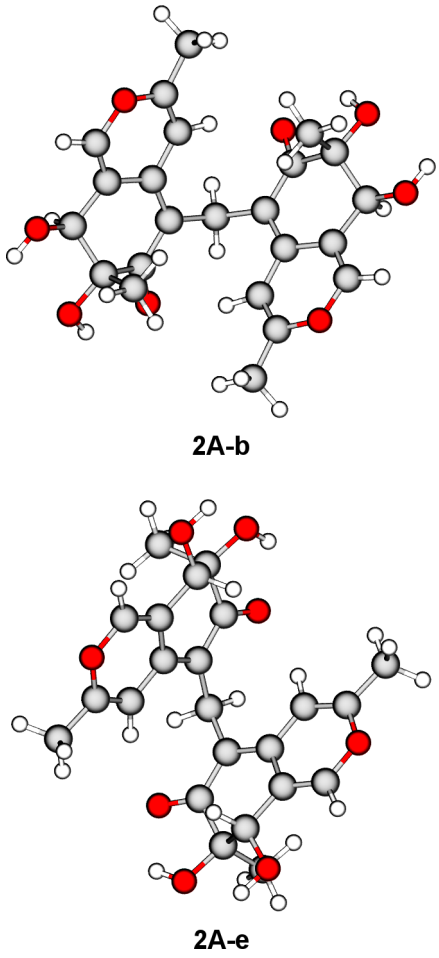

Figure 4. Most populated equilibrium conformers of **2A**.

DFT conformer **2A-b** shows a close resemblance to the crystallographic structure of **2**. On the basis of the foregoing evidence, the structure of mycoleptone A (**2**) was therefore elucidated as (7*R*,8*S*,7′*R*,8′*S*)-5-[(7′,8′-dihydroxy-3′,7′-dimethyl-6′-oxo-7′,8′-dihydro-6′*H*-isochromen-5′-yl)methyl]-7,8-dihydroxy-3,7-dimethyl-7,8-dihydro-6*H*-isochromen-6-one.

The molecular formula of mycoleptone B (**4**) was determined as $C_{23}H_{24}O_8$ by a combination of HRMS, ^{1}H and ^{13}C NMR, homonuclear correlation (COSY), heteronuclear multiple-quantum correlation (HMQC), and HMBC spectroscopies. The ^{1}H NMR spectrum contains five doublets, four singlets, two double doublets, and one multiplet; some similarities with the ^{1}H NMR spectrum of **2** are observed, with the presence of two hydrogen atoms on the pyran ring at δ_H 7.43 (1H, d, J = 1.8 Hz) and 6.63 (1H, s), an oxygenated sp^3 methine group at δ_H 4.42 (1H, d, J = 1.8 Hz), a CH_2 group at δ_H 3.60 (1H, d, J_{gem} = 15.0 Hz) and 3.53 (1H, d, J_{gem} = 15.0 Hz) due to the methylene bridge at position C-10 connecting the azaphilone unit to a dihydroisocoumarin moiety, and two methyl signals at δ_H 2.22 and 1.10. For the dihydroisocoumarin moiety, the ^{1}H NMR spectrum displays an oxygen-bearing methine hydrogen at δ_H 4.55 (1H, m), a methylene group at δ_H 3.17 (1H, dd, J = 16.0, 3.0 Hz) and 2.60 (1H, dd, J = 16.0, 11.0 Hz), and two methyl groups at δ_H 2.06 (3H, s) and 1.44 (3H, d, J = 6.2 Hz). The ^{13}C NMR spectrum of **4** displays signals for 23 carbon atoms: one signal due to the methylene bridge (δ_C 20.7), 11 signals belonging to the azaphilone moiety as in **2**,

Table 2. Geometric Parameters, Energy Values, and Fractional Equilibrium Populations for the Most Populated Equilibrium Conformers of the Diastereomers of Mycoleptone A, As Obtained after DFT Geometry Optimization at the B97D/6-311++G(2d,2p)/IEFPCM(MeOH) Level

	conformer	α_1 (deg)[a]	α_2 (deg)[b]	β (deg)[c]	d (Å)[d]	E_{QM} (Hartree)	ΔE_{QM} (kcal mol^{-1})	χ_{QM}[e]
2A	**2A-e**	−57.348	−57.348	−95.326	7.453	−1492.147 316 09	0.000	0.5934
	2A-b	66.788	66.788	101.136	7.806	−1492.146 929 07	0.243	0.3939
2B	**2B-f**	−56.583	−55.703	−92.428	7.308	−1492.149 394 96	0.000	0.6540
	2B-b	68.871	69.671	105.736	8.045	−1492.148 758 18	0.400	0.3332
2C	**2C-e**	62.947	57.866	94.503	7.444	−1492.149 386 42	0.000	0.5886
	2C-f	−60.999	−66.239	−101.552	7.806	−1492.149 010 68	0.236	0.3953
2D	**2D-b**	−68.275	−68.275	−104.848	8.007	−1492.150 185 72	0.000	0.9709

[a]C-10−C-5−C-12−C-5′ dihedral angle. [b]C-10′−C-5′−C-12−C-5 dihedral angle. [c]O-2−C-5−C-5′−O-2′ dihedral angle. [d]O-2−O-2′ distance. [e]Calculated using Boltzmann statistics at 298.15 K and 1 atm.

dx.doi.org/10.1021/np4006822 | J. Nat. Prod. 2014, 77, 70−78

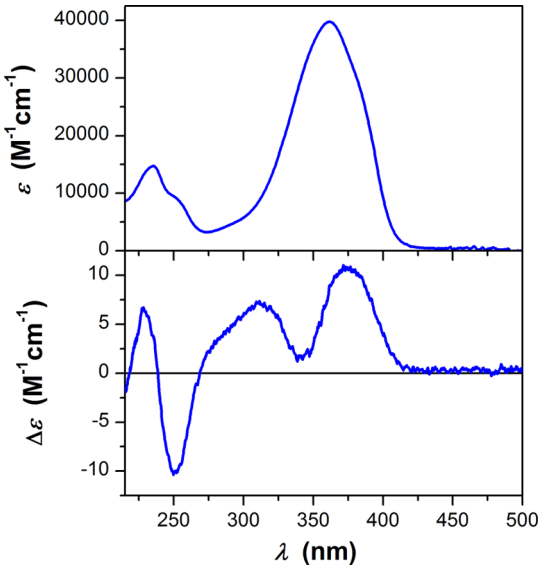

Figure 5. Experimental UV and ECD spectra of mycoleptone A (19 μM in MeOH, 1 cm path length).

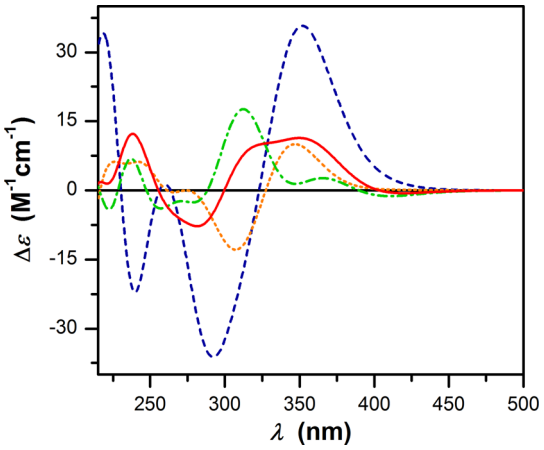

Figure 6. Theoretical ECD spectra of the diastereomers of mycoleptone A at the PBE0/6-311++G(2d,2p)/IEFPCM(MeOH)//B97D/6-311++G(2d,2p)/IEFPCM(MeOH) level (χ_{QM}-based conformational averaging, $\Delta\sigma$ = 0.3 eV). Solid: **2A**. Dash-dotted: **2B**. Dotted: **2C**. Dashed: **2D**.

and 11 signals belonging to the dihydroisocoumarin moiety. The ^{13}C NMR data reveal six resonances for sp^2 carbon atoms being part of a benzene ring, two of them characterized by a downfield shift due to the hydroxy substituents (C-6′ at δ_C 160.2; C-8′ at δ_C 160.9) and the presence of a carbonyl group at δ_C 171.2 (C-1′; IR ν_{max} 1652 cm^{-1}). The structural features of the lactone ring were determined from the ^{1}H−^{1}H COSY spectrum based on the couplings between H$_2$-4′ and H-3′, as well as between H-3′ and H$_3$-9′. The HMBC correlations of CH$_2$-4′ to δ_C 136.8 (C-5′), δ_C 100.1 (C-8a′), δ_C 75.0 (C-3′), and δ_C 19.6 (C-9′) proved the connection of the two units. In addition, the HMBC spectrum displays relevant correlations from CH$_2$-10 (δ_H 3.60, 3.53) to δ_C 199.3 (C-6), 143.7 (C-4a), and 112.8 (C-5) from the azaphilone moiety and to δ_C 160.9 (C-8′), 160.2 (C-6′), and 116.5 (C-7′) from the dihydroisocoumarin moiety, characterizing the connection between the two units by a methylene bridge to afford the compound (7*R*,8*S*)-5-[(6′,8′-dihydroxy-3′,5′-dimethyl-1′-oxoisochroman-7′-yl)methyl]-7,8-dihydroxy-3,7-dimethyl-7,8-dihydro-6*H*-isochromen-6-one.

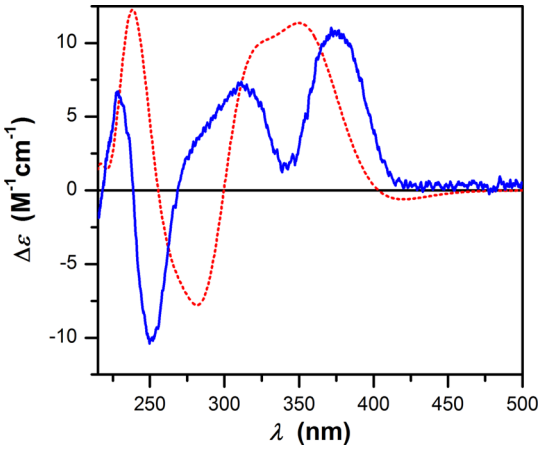

Figure 7. Theoretical ECD spectrum of **2A** and comparison with experimental data. Solid: experimental ECD spectrum of **2** (19 μM in MeOH, 1 cm path length). Dotted: theoretical ECD spectrum of **2A** at the PBE0/6-311++G(2d,2p)/IEFPCM(MeOH)//B97D/6-311++G(2d,2p)/IEFPCM(MeOH) level (χ_{QM}-based conformational averaging, $\Delta\sigma$ = 0.3 eV).

Table 3. Selected Bond Distances and Angles for Mycoleptone A and Austdiol, As Determined by X-ray Crystallography

parameter	mycoleptone A (**2**)	austdiol (**1**)
C-1−C-8a	1.337(8) Å	1.338(3) Å
C-3−C-4a	1.341(8) Å	1.345(3) Å
C-5−C-4a	1.373(7) Å	1.399(2) Å
C-5−C-6	1.433(8) Å	1.432(3) Å
C-5−C-10	1.533(7) Å	1.455(2) Å
C-4a−C-5−C-6	118.6(5)°	124.3(2)°

The molecular formula of mycoleptone C (**5**) was deduced as $C_{23}H_{22}O_8$ by HRMS analysis in combination with ^{1}H and ^{13}C NMR spectroscopies. The ^{1}H NMR spectrum displays nine singlets and two doublets; as in compounds **2** and **4**, the methylene group at δ_H 3.74 (1H, d, J = 15.0 Hz) and 3.46 (1H, d, J = 15.0 Hz) connects two moieties, the azaphilone and chromone units. The azaphilone moiety shows five uncoupled hydrogen atoms at δ_H 7.52 (H-1), 7.03 (H-4), 4.25 (H-8), 2.25 (H-9), and 1.00 (H-10); the chromone moiety displays four uncoupled hydrogen atoms at δ_H 13.06 (H-5′), 6.13 (H-3′), 2.37 (H-9′), and 2.00 (H-10′), the sharp singlet at δ_H 13.06 being interpreted as a hydrogen-bonded phenol hydroxy group. The ^{13}C NMR spectrum confirms 23 carbon signals, namely, four methyl, one methylene, four methine, and 14 quaternary carbon signals. The chromone moiety displays one ketone carbonyl group (δ_C 181.8; IR ν_{max} 1690 cm^{-1}) and four quaternary aromatic (δ_C 153.5, 107.8, 105.0, and 103.1), two oxygenated aromatic (δ_C 161.1 and 156.6), two unsaturated (δ_C 167.2 and 107.9), and two methyl (δ_C 20.2 and 8.5) carbon atoms. The structure of the chromone portion was determined on consideration of the molecular formula, double-bond equivalents, and the downfield shifts of the carbon signals at C-2′ and C-8a′ (δ_C 167.2 and 153.5). The HMBC spectrum of **5** revealed relevant correlations of CH$_2$-10 (δ_H 3.74, 3.46) to δ_C 200.5 (C-6), 144.3 (C-4a), and 112.1 (C-5) from the azaphilone moiety and to δ_C 161.1 (C-7′), 156.6 (C-5′), and 107.8 (C-6′) from the chromone moiety, revealing the

dx.doi.org/10.1021/np4006822 | J. Nat. Prod. 2014, 77, 70−78

connection of both skeletons and featuring **5** as (7*R*,8*S*)-5-[(5′,7′-dihydroxy-2′,8′-dimethyl-4′-oxo-4′*H*-chromen-6′-yl)-methyl]-7,8-dihydroxy-3,7-dimethyl-7,8-dihydro-6*H*-isochromen-6-one.

The presence of a methylene bridge is very uncommon among natural compounds, and only a few azaphilone dimers have been reported showing such a feature.[15] Dicitrinones A–C[23] were isolated from *Penicillium citrinum*, a volcano ash-derived fungus: the presence of a single sp^3 carbon bridge, either a methine or methylene group, was proposed to derive from the carboxyl group of citrinin through decarboxylation, reduction, and Friedel–Crafts alkylation mediated by a polyketide biosynthetic pathway. The methylene bridge in aspergilone B,[24] an azaphilone dimer that was isolated from a marine-derived fungus of the *Aspergillus* species, was hypothesized to derive from a formaldehyde biosynthetic pathway; the same hypothesis was proposed for the biosynthesis of xyloketal F,[25] a dimer isolated from a mangrove fungus of the *Xylaria* species.

The condensation of two austdiol units to form mycoleptone A (**2**) is consistent with a possible biosynthetic pathway similar to the one proposed for dicitrinone C[23] (Figure 8). One austdiol unit may undergo decarbonylation, while the aldehyde group of the second austdiol unit may be reduced to a reactive carbocation species: the two units may then react by Friedel–Crafts alkylation. Similar pathways may also explain the condensation of the dihydroisocoumarin and chromone units with an austdiol unit in mycoleptones B (**4**) and C (**5**), respectively. Due to the limited number of methylene-bridged azaphilones discovered to date, however, a general biosynthetic pathway cannot be postulated, and the biologically mediated mechanisms of such reactions are unknown.

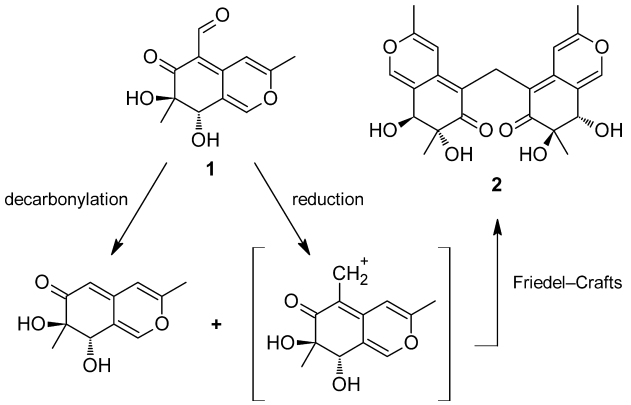

Figure 8. Possible pathway for the biosynthesis of mycoleptone A.

The results of antileishmanial and cytotoxicity tests on the isolated compounds are shown in Table 4. Compounds **1**–**9** exhibit no significant activity against *Leishmania donovani* and *Leishmania major* compared to the standard antileishmanial drugs Geneticin (*L. major*), amphotericin B, and pentamidin (*L. donovani*). Mycoleptone B (**4**) was the most cytotoxic metabolite (PC3 cells: IC_{50} = 7.1 ± 3.8 μM), but its activity was lower than that of doxorubicin, the reference compound for cytotoxicity assays.

EXPERIMENTAL SECTION

General Experimental Procedures. Optical rotations were measured in $CHCl_3$, MeOH, or DMSO using a Jasco DIP-370 digital polarimeter at room temperature; IR spectra were recorded with KBr discs using a Bruker Tensor 27 FTIR spectrometer. UV spectra were measured in $CHCl_3$, MeOH, and DMSO on a Varian Cary 50 Bio UV–visible spectrophotometer. The HPLC system consisted of a Shimadzu SCL-10Avp multisolvent delivery system, a SPD-M10Avp photodiode array detector, an Intel Celeron computer for analytical system control, data collection, and processing, and a Shim-pack CLC-ODS(M) reversed-phase column (250 × 4.5 mm i.d.; 5 μm particle size) protected by a Pelliguard LC-18 cartridge. The NMR spectra were acquired on a Bruker Avance DRX-400 spectrometer operating at 400 MHz for ^1H NMR and 100 MHz for ^{13}C NMR in $CDCl_3$, CD_3OD, or DMSO-d_6; multiplicity determinations (DEPT) and 2D NMR spectra (COSY, HMQC, and HMBC) were obtained using standard Bruker pulse programs. The chemical shift values (δ) are given in parts per million (ppm), and the coupling constants are in Hz. HRMS were obtained by direct injection using a Bruker Bioapex FTMS spectrometer with electrospray ionization (ESI). UV and ECD spectra of **2** in MeOH (sample concentration: 19 μM) were recorded in the 500–215 nm spectral range on a Jasco J-810 spectropolarimeter, using a 1 cm path length cell at room temperature: measurements

Table 4. Biological Activities of Compounds 1–9

			cytotoxicity (IC_{50}, μM)					
compound	*L. major* (LD_{50}, μM)	*L. donovani* (IC_{50}, μM)	HCT-8	HL-60	MDA-MB435	PC3	SF-295	human lymphocyte
austdiol (**1**)	20.5	80.5	12.9 ± 3.5	38.8 ± 9.3	34.3 ± 4.3	ND	28.0 ± 7.2	>113
mycoleptone A (**2**)	28.5	>93.4	>58	>58	>58	10.0 ± 6.5	>58	>58
eugenitin (**3**)	39.9	>181	>113	>113	>113	>113	>113	>113
mycoleptone B (**4**)	21.7	ND[d]	>58	>58	>58	7.1 ± 3.8	>58	>58
mycoleptone C (**5**)	ND	ND	ND	ND	ND	ND	ND	ND
6-methoxyeugenin (**6**)	34.5	>169	>105	>105	>105	20.5 ± 11.9	>105	>105
9-hydroxyeugenin (**7**)	ND	ND	>105	>105	>105	>105	>105	>105
austdiol diacetate (**8**)	19.8	59.3	13.9 ± 2.6	22.1 ± 2.6	26.9 ± 0.3	ND	26.3 ± 1.2	>78
mycoleptone A tetraacetate (**9**)	ND	ND	>42	>42	>42	33.3 ± 29.0	>42	>42
Geneticin (G418)[a]	3.43							
pentamidine[b]		0.0041						
amphotericin B[b]		0.140						
doxorubicin[c]			0.10 ± 0.01	0.05 ± 0.01	1.51 ± 0.20	0.41 ± 0.05	0.70 ± 0.20	0.70 ± 0.20

[a]Standard antileishmanial drug against *L. major*. [b]Standard antileishmanial drugs against *L. donovani*. [c]Reference compound for cytotoxicity assays. [d]ND: not determined.

dx.doi.org/10.1021/np4006822 | *J. Nat. Prod.* 2014, 77, 70–78

were carried out at 0.2 nm intervals using a 1 nm spectral bandwidth, a 20 nm min^{-1} scan rate, and a 4 s time constant.

Fungal Material. The fungus was isolated as an endophyte from the medicinal plant *Borreria verticillata* (L.) G. F. W. Meyer, belonging to the Rubiaceae family, and is native to South America. Five specimens of *B. verticillata* with a healthy appearance were collected from the campus of the Federal University of Pernambuco (UFPE) (34°56′57″ W; 8°2′53″ S) in January 2006, approximately 43 cm in height and bearing flowers. Then, the samples were taken to the laboratory and processed in 24 h. A voucher specimen of the plant (No. 42.234/UFPE) was identified and deposited at the Herbarium Professor Geraldo Mariz, UFP, Department of Botany, UFPE, Recife, Brazil. The isolate was identified as *Mycoleptodiscus indicus* based on sequence analysis of the ITS region of the rDNA (GenBank accession number GU220382.1).

Cultivation, Extraction, and Isolation. *M. indicus* was grown on potato dextrose agar plates for 7 days at 30 °C. Then, 10 plugs were transferred to five Erlenmeyer flasks (500 mL), each containing 100 mL of potato dextrose broth prepared with distilled water. Flasks were shaken on a rotary shaker at 30 °C and 120 rpm for 48 h. Next, 10 mL was transferred to each of 50 flasks containing 90 g of solid medium (rice-oat). These were grown for 30 days. On day 30, the mycelial mass was macerated with ethanol overnight and filtered. The filtrate was concentrated under vacuum to obtain a crude ethanol extract (22 g), which was partitioned with three times equal volumes of hexane and CH_2Cl_2, respectively, yielding hexane (6 g) and dichloromethane fractions (6.9 g). The CH_2Cl_2 fraction was suspended in MeOH and centrifuged at 3000 rpm for 3 min, furnishing a precipitate fraction (3870 mg) and a soluble fraction (3030 mg). The precipitate fraction was subjected to chromatography over a silica gel column (30 × 3.5 cm i.d.) using a MeOH−CH_2Cl_2 gradient to yield 67 fractions, which were combined on the basis of their TLC profiles into seven fractions: A (19 mg), B (33 mg), C (2968 mg), D (100 mg), E (210 mg), F (285 mg), and G (109 mg). Fraction C (2968 mg) yielded austdiol (2830 mg), after crystallization in MeOH, and fraction E afforded mycoleptone A (**2**, 200 mg) by precipitation. The soluble fraction (3030 mg) was subjected to gel filtration on a Sephadex LH-20 column (50 × 3 cm i.d.) using MeOH as the mobile phase, furnishing 10 fractions (S1−S10). Fraction S6 (280 mg) was washed with MeOH, yielding eugenitin (50 mg). The soluble portion was subjected to chromatography over a silica gel column (25 × 2 cm i.d.) using a MeOH−CH_2Cl_2 gradient. Forty-two fractions were collected and combined on the basis of their TLC profiles to yield nine fractions. The fourth fraction (S6.4, 28 mg) was purified by preparative silica gel TLC using hexane−ethyl acetate (70:30, v/v) as eluent to furnish mycoleptone B (**4**, 10 mg) and mycoleptone C (**5**, 2 mg). Fraction S5 (461 mg) was subjected to chromatography over a silica gel column (25 × 2 cm i.d.) eluted with a gradient of MeOH in CH_2Cl_2. Thirty fractions were collected and combined on the basis of their TLC profiles to yield 10 fractions. The fourth fraction (S5.4, 60 mg) was purified by preparative silica gel TLC using hexane−ethyl acetate (70:30, v/v) as eluent to provide 6-methoxyeugenin (14 mg). The fifth fraction (S5.5, 4 mg) was subjected to reversed-phase HPLC using CH_3CN−H_2O (10:90 to 100:0, v/v) as mobile phase at a flow rate of 1.0 mL/min over 23 min, yielding 9-hydroxyeugenin (2 mg).

Acetylation of Austdiol and Mycoleptone A (2). A solution containing austdiol (80 mg), pyridine (2 mL), and Ac_2O (3 mL) was stirred at room temperature for 8 h. H_2O (6 mL) was added into the reaction mixture, which was subsequently extracted with CH_2Cl_2. The organic layer was evaporated to give a yellow, amorphous solid (140 mg), which was purified by preparative TLC eluted with a mixture of CH_2Cl_2−MeOH (98:2, v/v) to afford the diacetylated derivative (**8**, 80.7 mg). Acetylation of mycoleptone A (**2**, 25 mg) was performed in a similar manner, yielding the tetraacetylated derivative (**9**, 20 mg).

Quantum-Mechanical Calculations. Conformational analysis on the selected diastereomers of **2** was performed in two steps. In the first step, a preliminary conformer distribution was determined by molecular mechanics (MM) calculations at the MMFF94s[26] level using the Spartan'02 software.[27] In the second step, DFT[28,29] geometry optimizations were performed on the MM conformers having relative energies (ΔE_{MM}) within a threshold value of 3 kcal mol^{-1}. DFT calculations were carried out at the B97D/6-311++G(2d,2p) level[30−33] using the Gaussian 09 software package.[34] The Boltzmann distribution of conformers at 298.15 K and 1 atm was then calculated from the relative electronic energies (ΔE_{QM}). TD-DFT[35] calculations were carried out at the PBE0/6-311++G(2d,2p) level[31−33,36−38] using the Gaussian 09 software package.[34] All calculations were performed using the IEFPCM continuum solvation model[39,40] for MeOH. Rotational strengths (R_j) and excitation wavelengths (λ_j) were calculated for the lowest 50 excited states on the optimized geometries having $\Delta E_{QM} \leq 2$ kcal mol^{-1}. Theoretical ECD spectra were then obtained by approximation of R_j values to Gaussian functions with a half-bandwidth at $\Delta\varepsilon_{max}/e$ ($\Delta\sigma$) of 0.3 eV, summation over all excited states, and conformational averaging, according to the Boltzmann distribution of conformers (χ_{QM}).[41]

Crystallographic Structure. Crystals of **2** suitable for X-ray analysis were obtained by crystallization from a methanol solution. A colorless prismatic crystal of approximate dimensions 0.3 × 0.2 × 0.2 mm^3 was used for the experiment. X-ray data were measured on an Enraf-Nonius CAD-4 diffractometer employing graphite-monochromated Cu Kα radiation (λ = 1.5418 Å) at 298 K and operating in the $\varphi-\omega$ scan mode. Crystal data: $C_{23}H_{24}O_8$, M = 428.42, triclinic, space group $P1$, a = 10.473(6) Å, b = 11.223(3) Å, c = 11.429(2) Å, α = 60.65(2)°, β = 89.83(3)°, γ = 67.75(4)°, V = 1055.5(9) $Å^3$, Z = 2, D_c = 1.348 g/cm^3, $F(000)$ = 452, and μ(Cu Kα) = 0.86 mm^{-1}. All tested crystal samples showed gemination, and the sample used for data collection was visually homogeneous, but it showed pseudomerohedral twinning, which caused partial superposition of structure factors leading to high residuals during the structure refinements. A total of 8384 reflections were collected (4273 unique plus 96.2% of Friedel mates) in the θ range 4.56° to 73.92° and index ranges h from 15 to −15, k from −24 to 25, and l from −15 to 15. Cell refinement and data reduction were performed with the XCAD4 software suite. The structure was solved and refined using the WingX with SHELX97 suite.[42,43] Structure refinement was performed on F^2 by full-matrix least-squares calculations. Non-hydrogen atoms were refined anisotropically, and all hydrogen atoms were placed in idealized coordinates and refined as riding atoms with isotropic parameters relative to their parent atoms. The final refinement residuals were R_1 = 0.091 (wR_2 = 0.32) for 6964 observed reflections with $I > 2\sigma(I)$, 575 variable parameters, and three restraints, being R_1 = 0.11 (wR_2 = 0.32) for all unique reflections with GoF = 1.41. The absolute structure Flack parameter was 0.1(3), indicating that the chiral sense was correctly chosen, although this number was not reliable, given the large standard deviation, in the absence of strong anomalous scatterers.

Biological Assays. The microplate Alamar-Blue assay was used to determine growth inhibition against *L. donovani*.[44] Antileishmanial (*L. major*) and cytotoxicity assays against human colon cancer (HCT-8) cells, human leukemia cancer (HL-60) cells, human melanoma cancer (MDA-MB435) cells, human prostate cancer (PC3) cells, human glioblastoma cancer (SF-95) cells, and human lymphocyte cells were assessed employing a colorimetric method.[45]

Austdiol (1): yellow crystal; mp 255−257 °C; $[\alpha]^{25}_D$ +223 (*c* 1.0, DMSO); UV (MeOH) λ_{max} (log ε) 212 (2.64), 255 (2.57), 333 (2.62) nm; IR (KBr) ν_{max} 3470, 3373, 3100, 1679, 1604, 1471 cm^{-1}; ^{1}H NMR and ^{13}C NMR reported in the Supporting Information; HRMS *m/z* 237.0759 $[M + H]^+$ (calcd for $C_{12}H_{12}O_5 + H^+$, 237.0757).

Mycoleptone A (2): yellow crystal; mp 307−308 °C; $[\alpha]^{25}_D$ +351 (*c* 1.0, DMSO); UV (MeOH) λ_{max} (log ε) 254 (2.90), 361 (2.83) nm; IR (KBr) ν_{max} 3360, 1667, 1581, 1526, 1229, 1197, 1090, 878 cm^{-1}; ^{1}H and ^{13}C NMR reported in Table 1; HRMS *m/z* 429.1543 $[M + H]^+$ (calcd for $C_{23}H_{24}O_8 + H^+$, 429.1544).

Eugenitin (3): White, solid powder; mp 153−156 °C; $[\alpha]^{25}_D$ 0 (*c* 0.3, $CHCl_3$); UV (MeOH) λ_{max} (log ε) 267 (2.53), 307 (2.55), 338 (2.54) nm; IR (KBr) ν_{max} 1652, 1586, 1435, 1338, 1179 cm^{-1}; ^{1}H NMR and ^{13}C NMR reported in the Supporting Information; HRMS *m/z* 221.0810 $[M + H]^+$ (calcd for $C_{12}H_{12}O_4 + H^+$, 221.0808).

Mycoleptone B (4): colorless, amorphous solid; $[\alpha]^{25}_D$ +71 (*c* 0.2, MeOH); UV (MeOH) λ_{max} (log ε) 237 (2.83), 299 (2.83), 317 (2.90) nm; IR (KBr) ν_{max} 3391, 2925, 1652, 1615, 1289, 1127 cm^{-1}; ^{1}H and

dx.doi.org/10.1021/np4006822 | J. Nat. Prod. 2014, 77, 70−78

^{13}C NMR reported in Table 1; HRMS *m/z* 451.1363 $[M + Na]^+$ (calcd for $C_{23}H_{24}O_8 + Na^+$, 451.1363).

*Mycoleptone C (**5**):* brown, amorphous solid; $[\alpha]^{25}_D$ +95 (*c* 0.2, DMSO); UV (MeOH) λ_{max} (log ε) 224 (3.17), 297 (3.15), 321 (3.17) nm; IR (KBr) ν_{max} 2920, 2360, 1690, 1573, 1478 cm^{-1}; ^{1}H and ^{13}C NMR reported in Table 1; HRMS *m/z* 427.1387 $[M + H]^+$ (calcd for $C_{23}H_{22}O_8 + H^+$, 427.1387).

*6-Methoxyeugenin (**6**):* white, solid powder; mp 155−158 °C; $[\alpha]^{25}_D$ 0 (*c* 0.3, $CHCl_3$); UV (MeOH) λ_{max} (log ε) 292 (2.85), 307 (2.89), 334 (2.88) nm; IR (KBr) ν_{max} 3404, 2923, 1657, 1617, 1570, 1492, 1169 cm^{-1}; ^{1}H NMR and ^{13}C NMR reported in the Supporting Information; HRMS *m/z* 259.0577 $[M + Na]^+$ (calcd for $C_{12}H_{12}O_5 + Na^+$, 259.0577).

*9-Hydroxyeugenin (**7**):* white, amorphous solid; $[\alpha]^{25}_D$ 0 (*c* 0.3, $CHCl_3$); UV (MeOH) λ_{max} (log ε) 279 (2.87), 319 (2.91), 335 (2.92) nm; IR (KBr) ν_{max} 3217, 2360, 1662, 1573, 1497, 1330, 1138 cm^{-1}; ^{1}H NMR and ^{13}C NMR reported in the Supporting Information; HRMS *m/z* 237.0711 $[M + H]^+$ (calcd for $C_{12}H_{12}O_5 + H^+$, 237.0757).

*Austdiol diacetate (**8**):* yellow crystal; mp 255−257 °C; $[\alpha]^{25}_D$ +39 (*c* 1.0, $CDCl_3$); UV ($CHCl_3$) λ_{max} (log ε) 262 (2.99), 281 (2.98), 362 (3.01) nm; IR (KBr) ν_{max} 2946, 1746, 1628, 1500, 1241 cm^{-1}; ^{1}H NMR and ^{13}C NMR reported in the Supporting Information; HRMS *m/z* 321.0970 $[M + H]^+$ (calcd for $C_{16}H_{16}O_7 + H^+$, 321.0969).

*Mycoleptone A tetraacetate (**9**):* white crystal; mp 260−263 °C; $[\alpha]^{25}_D$ +159 (*c* 1.0, $CDCl_3$); UV (MeOH) λ_{max} (log ε) 285 (3.04), 328 (2.98), 343 (3.03) nm; IR (KBr) ν_{max} 3470, 3373, 3100, 1679, 1604 cm^{-1}; ^{1}H NMR ($CDCl_3$, 400 MHz) δ 6.95 (1H, d, H-1), 6.71 (1H, d, H-8), 6.27 (1H, s, H-4), 3.48 (2H, s, H-10), 2.20 (3H, s, 7-$COOCH_3$), 2.18 (3H, s, H-9), 2.04 (3H, s, 8-$COOCH_3$), 1.32 (3H, s, H-11); ^{13}C NMR ($CDCl_3$, 100 MHz) δ 190.5 (C, CO), 169.7 (C, 7-CO_2Me), 169.5 (C, 8-CO_2Me), 160.0 (C, C-3), 142.6 (CH, C-1), 142.3 (C, C-4a), 117.3 (C, C-8a), 114.6 (C, C-5), 106.1 (CH, C-4), 82.5 (C, C-7), 69.1 (CH, C-8), 19.5 (CH_3, C-9), 20.8 (CH_3, 7-CO_2CH_3), 21.4 (CH_3, 8-CO_2CH_3), 17.2 (CH_2, C-10); HRMS *m/z* 597.1966 (calcd for $C_{31}H_{32}O_{12} + H^+$, 597.1967).

■ ASSOCIATED CONTENT

Ⓢ Supporting Information

NMR and HRMS spectra; results for the computational study on mycoleptone A. This material is available free of charge via the Internet at http://pubs.acs.org. Crystallographic data, excluding structure factors, have been deposited with the Cambridge Crystallographic Data Centre as supplementary publication number CCDC 938460. Copies of the data can be obtained, free of charge, on application to CCDC, 12 Union Road, Cambridge CB2 1EZ, UK [fax: C44 1223 336033 or e-mail: deposit@ccdc.cam.ac.uk].

■ AUTHOR INFORMATION

Corresponding Author

*Tel: +5516 3602 4162. Fax: +5516 3633 1092. E-mail: jkbastos@fcfrp.usp.br.

Notes

The authors declare no competing financial interest.

■ ACKNOWLEDGMENTS

The authors thank the São Paulo Research Foundation (FAPESP) grant nos. 04/07935-6 and 07/58650-0, CAPES, CNPq, the PRIN 2008 project 2008LYSEBR_005 (MIUR, Italy), and the University of Bologna for financial support.

■ REFERENCES

(1) Petrini, O. In *Microbial Ecology of Leaves*; Andrews, J. H., Hirano, S. S., Eds.; Springer-Verlag: New York, NY, 1991; pp 179−197.
(2) Gunatilaka, A. A. L. *J. Nat. Prod.* **2006**, *69*, 509−526.
(3) Borges, W. S.; Borges, K. B.; Bonato, P. S.; Said, S.; Pupo, M. T. *Curr. Org. Chem.* **2009**, *13*, 1137−1163.
(4) Bunyapaiboonsri, T.; Yoiprommarat, S.; Srikitikulchai, P.; Srichomthong, K.; Lumyong, S. *J. Nat. Prod.* **2010**, *73*, 55−59.
(5) Shearer, J. F. *J. Aquat. Plant Manage.* **2002**, *40*, 76−78.
(6) Padhye, A. A.; Davis, M. S.; Reddick, A.; Bell, M. F.; Gearhart, E. D.; Von Moll, L. *J. Clin. Microbiol.* **1995**, *33*, 2796−2797.
(7) Garrison, A. P.; Procop, G. W.; Vincek, V.; Moon, J.; Morris, M. I.; Doblecki-Lewis, S.; Cleary, T. J.; Brust, D.; Rosa-Cunha, I. *Transpl. Infect. Dis.* **2008**, *10*, 218−220.
(8) Steyn, P. S. *Tetrahedron* **1973**, *29*, 107−120.
(9) Vleggaar, R.; Steyn, P. S.; Nagel, D. W. *J. Chem. Soc., Perkins Trans. 1* **1974**, 45−49.
(10) Feng, Y.; Blunt, J. W.; Cole, A. L. J.; Munro, M. H. G. *J. Nat. Prod.* **2002**, *65*, 1681−1682.
(11) Fox, C. H.; Huneck, S. *Phytochemistry* **1969**, *8*, 1301−1304.
(12) Joshi, B. S.; Ravindranath, K. R. *J. Chem. Soc., Perkin Trans. 1* **1977**, 433−436.
(13) Li, G. Y.; Li, B. G.; Yang, T.; Liu, G. Y.; Zhang, G. L. *Helv. Chim. Acta* **2008**, *91*, 124−129.
(14) Osmanova, N.; Schultze, W.; Ayoub, N. *Phytochem. Rev.* **2010**, *9*, 315−342.
(15) Gao, J. M.; Yang, S. X; Qin, J. C. *Chem. Rev.* **2013**, *113*, 4755−4811.
(16) Arai, N.; Shiomi, K.; Tomoda, H.; Tabata, N.; Yang, D. J.; Masuma, R.; Kawakubo, T.; Omura, S. *J. Antibiot.* **1995**, *48*, 696−702.
(17) Colombo, L.; Gennari, C.; Severini Ricca, G.; Scolastico, C.; Aragozzini, F. *J. Chem. Soc., Chem. Commun.* **1981**, 575−576.
(18) Park, J. H.; Choi, G. J.; Jang, K. S.; Lim, H. K.; Kim, H. T.; Cho, K. Y.; Kim, J. C. *FEMS Microbiol. Lett.* **2005**, *252*, 309−313.
(19) Autschbach, J. *Chirality* **2009**, *21*, E116−E152.
(20) Polavarapu, P. L. *Chirality* **2012**, *24*, 909−920.
(21) Goerigk, L.; Kruse, H.; Grimme, S. In *Comprehensive Chiroptical Spectroscopy*; Berova, N.; Polavarapu, P. L.; Nakanishi, K.; Woody, R. W., Eds.; Wiley & Sons: Hoboken, NJ, 2012; Vol. *1*, pp 643−673.
(22) Lo Presti, L.; Soave, R.; Destro, R. *Acta Crystallogr.* **2003**, *C59*, o199−o201.
(23) Du, L.; Li, D.; Zhang, G.; Zhu, T.; Ai, J.; Gu, Q. *Tetrahedron* **2010**, *66*, 9286−9290.
(24) Shao, C. L.; Wang, C. Y.; Wei, M. Y.; Gu, Y. C.; She, Z. G.; Qian, P. Y; Lin, Y. C. *Bioorg. Med. Chem. Lett.* **2011**, *21*, 690−693.
(25) Wu, X. Y.; Liu, X. H.; Lin, Y. C.; Luo, J. H.; She, Z. G.; Houjin, L.; Chan, W. L.; Antus, S.; Kurtan, T.; Elsässer, B.; Krohn, K. *Eur. J. Org. Chem.* **2005**, *2005*, 4061−4064.
(26) Halgren, T. A. *J. Comput. Chem.* **1999**, *20*, 720−729.
(27) *Spartan'02*; Wavefunction, Inc.: Irvine, CA, 2002.
(28) Hohenberg, P.; Kohn, W. *Phys. Rev.* **1964**, *136*, B864−B871.
(29) Kohn, W.; Sham, L. J. *Phys. Rev.* **1965**, *140*, A1133−A1138.
(30) Grimme, S. *J. Comput. Chem.* **2006**, *27*, 1787−1799.
(31) Krishnan, R.; Binkley, J. S.; Seeger, R.; Pople, J. A. *J. Chem. Phys.* **1980**, *72*, 650−654.
(32) Clark, T.; Chandrasekhar, J.; Spitznagel, G. W.; Schleyer, P. V. R. *J. Comput. Chem.* **1983**, *4*, 294−301.
(33) Frisch, M. J.; Pople, J. A.; Binkley, J. S. *J. Chem. Phys.* **1984**, *80*, 3265−3269.
(34) Frisch, M. J.; Trucks, G. W.; Schlegel, H. B.; Scuseria, G. E.; Robb, M. A.; Cheeseman, J. R.; Scalmani, G.; Barone, V.; Mennucci, B.; Petersson, G. A.; Nakatsuji, H.; Caricato, M.; Li, X.; Hratchian, H. P.; Izmaylov, A. F.; Bloino, J.; Zheng, G.; Sonnenberg, J. L.; Hada, M.; Ehara, M.; Toyota, K.; Fukuda, R.; Hasegawa, J.; Ishida, M.; Nakajima, T.; Honda, Y.; Kitao, O.; Nakai, H.; Vreven, T.; Montgomery, J. A., Jr.; Peralta, J. E.; Ogliaro, F.; Bearpark, M.; Heyd, J. J.; Brothers, E.; Kudin, K. N.; Staroverov, V. N.; Kobayashi, R.; Normand, J.; Raghavachari, K.; Rendell, A.; Burant, J. C.; Iyengar, S. S.; Tomasi, J.; Cossi, M.; Rega, N.; Millam, J. M.; Klene, M.; Knox, J. E.; Cross, J. B.; Bakken, V.; Adamo, C.; Jaramillo, J.; Gomperts, R.; Stratmann, R. E.; Yazyev, O.; Austin, A. J.; Cammi, R.; Pomelli, C.; Ochterski, J. W.; Martin, R. L.; Morokuma, K.; Zakrzewski, V. G.; Voth, G. A.; Salvador, P.; Dannenberg, J. J.; Dapprich, S.; Daniels, A. D.; Farkas, Ö.;

Foresman, J. B.; Ortiz, J. V.; Cioslowski, J.; Fox, D. J. *Gaussian 09*, Revision A.02; Gaussian, Inc.: Wallingford, CT, 2009.
(35) Bauernschmitt, R.; Ahlrichs, R. *Chem. Phys. Lett.* **1996**, *256*, 454−464.
(36) Perdew, J. P.; Burke, K.; Ernzerhof, M. *Phys. Rev. Lett.* **1996**, *77*, 3865−3868.
(37) Perdew, J. P.; Burke, K.; Ernzerhof, M. *Phys. Rev. Lett.* **1997**, *78*, 1396.
(38) Adamo, C.; Barone, V. *J. Chem. Phys.* **1999**, *110*, 6158−6169.
(39) Tomasi, J.; Mennucci, B.; Cancès, E. *J. Mol. Struct. (THEOCHEM)* **1999**, *464*, 211−226.
(40) Tomasi, J.; Mennucci, B.; Cammi, R. *Chem. Rev.* **2005**, *105*, 2999−3093.
(41) Stephens, P. J.; Harada, N. *Chirality* **2010**, *22*, 229−233.
(42) Farrugia, L. J. *J. Appl. Crystallogr.* **1999**, *32*, 837−838.
(43) Sheldrick, G. M. *Acta Crystallogr.* **2008**, *A64*, 112−122.
(44) Mikus, J.; Steverding, D. *Parasitol. Int.* **2000**, *48*, 265−269.
(45) Mosmann, T. *J. Immunol. Methods* **1983**, *65*, 55−63.